

Serveur Académique Lausannois SERVAL serval.unil.ch

Author Manuscript

Faculty of Biology and Medicine Publication

This paper has been peer-reviewed but does not include the final publisher proof-corrections or journal pagination.

Published in final edited form as:

Title: Plasmacytoid dendritic cells are productively infected and activated through TLR-7 early after arenavirus infection.

Authors: Macal M, Lewis GM, Kunz S, Flavell R, Harker JA, Zúñiga EI

Journal: Cell host & microbe

Year: 2012 Jun 14

Volume: 11

Issue: 6

Pages: 617-30

DOI: 10.1016/j.chom.2012.04.017

In the absence of a copyright statement, users should assume that standard copyright protection applies, unless the article contains an explicit statement to the contrary. In case of doubt, contact the journal publisher to verify the copyright status of an article.

Published in final edited form as:

Cell Host Microbe. 2012 June 14; 11(6): 617–630. doi:10.1016/j.chom.2012.04.017.

Plasmacytoid Dendritic Cells Are Productively Infected And Activated Through TLR-7 Early After Arenavirus Infection

Monica Macal¹, Gavin M. Lewis¹, Stefan Kunz³, Richard Flavell², James A. Harker¹, and Elina I. Zuñiga^{1,*}

¹Division of Biological Sciences, University of California San Diego, La Jolla, San Diego, CA, USA

²Department of Immunobiology, Yale University School of Medicine, New Haven, CT, USA

³Institute of Microbiology, University Hospital Center and University of Lausanne, Lausanne, Switzerland

SUMMARY

The antiviral response is largely mediated by dendritic cells (DC), including conventional (c) DCs that function as antigen presenting cells and plasmacytoid (p) DCs that produce Type I interferons, making them an attractive target for viruses. We find that the Old-world arenaviruses lymphocytic choriomeningitis virus clone 13 (LCMV Cl13) and Lassa virus bind pDCs to a greater extent than cDCs. Consistently, LCMV Cl13 targets pDCs early after *in vivo* infection of its natural murine host and establishes a productive and robust replication cycle. pDCs co-produce type I interferons and pro-inflammatory cytokines, with the former being induced in both infected and uninfected pDCs, demonstrating a dissociation from intrinsic virus replication. TLR7 globally mediates pDC responses, limits pDC viral load and promotes rapid innate and adaptive immune cell activation. These early events likely help dictate the outcome of infections with arenaviruses and other DC-replicating viruses and shed light on potential therapeutic targets.

Keywords

dendritic cell; plasmacytoid dendritic cells; type I interferon; interleukin-12; innate; toll like receptor-7; lymphocytic choriomeningitis virus (LCMV); Lassa Fever virus (LASV); arenavirus; chronic viral infection

INTRODUCTION

Dendritic cells (DC) are a heterogeneous population, exhibiting unique and overlapping functions in the orchestration of immune responses. Conventional DCs (cDCs) can be

© 2012 Elsevier Inc. All rights reserved.

*Corresponding author: Elina I. Zuniga, Division of Biological Sciences, University of California San Diego, 3110 Bonner Hall, 9500 Gilman Drive, La Jolla, San Diego, CA. Phone: (858) 5345660. Fax (858) 822-3021 eizuniga@ucsd.edu.

AUTHORS CONTRIBUTION

M.M. designed, performed, analyzed and interpreted all experiments described; G.M.L. helped design, perform and interpret antigen presentation assays; S.K. contributed to the design, interpretation and performance of virus binding assays; R.F. generated the TLR7^{-/-} mice; J.A.H. helped design, perform and interpret the immunofluorescence microscopy; E.Z. helped perform initial experiments and oversaw the design, analysis and interpretation of all studies described. M.M. and E.Z. wrote the manuscript.

Publisher's Disclaimer: This is a PDF file of an unedited manuscript that has been accepted for publication. As a service to our customers we are providing this early version of the manuscript. The manuscript will undergo copyediting, typesetting, and review of the resulting proof before it is published in its final citable form. Please note that during the production process errors may be discovered which could affect the content, and all legal disclaimers that apply to the journal pertain.

subdivided into CD11b⁺ and CD11b⁻ (CD8⁺) cDCs and function as professional antigen presenting cells (Banchereau and Steinman, 1998; Shortman, 2000). In contrast, plasmacytoid DCs (pDC) are specialized to produce large amounts of the antiviral mediator, type I interferon (IFN-I), and synthesize a broad range of IFN-I isoforms following microbial stimulation (Reizis et al., 2011; Swiecki and Colonna). pDCs exert multiple other functions, including IL-12 production, which along with IFN-I, can activate natural killer (NK) and T cells (Swiecki and Colonna). Because IFN-I can inhibit IL-12 production (Cousens et al., 1997; McRae et al., 1998), it is possible that distinct, mutually exclusive, pDC maturation stages or subtypes secrete these cytokines. pDCs can also present antigens during infection with several viruses, albeit not as powerfully as cDCs (Villadangos and Young, 2008). Finally, pDCs are infected by human immunodeficiency virus (HIV) (Fitzgerald-Bocarsly and Jacobs, 2010) and can uptake hepatitis B virus (HBV) (Untergasser et al., 2006), but the functional consequences of these events remain unclear. In sum, pDCs play important roles in both innate and adaptive immune responses, and understanding the interactions between pDCs and viruses is of great significance.

Arenaviruses include several causative agents of severe hemorrhagic fevers in humans, causing hundreds of thousands of disease cases each year in Africa and South America, as well as lymphocytic choriomeningitis virus (LCMV), a prevalent human pathogen with worldwide distribution (McCormick and Fisher-Hoch, 2002; Oldstone, 2002). New pathogenic arenaviruses are continuously emerging (Geisbert and Jahrling, 2004) and, with no licensed vaccines, only limited treatments available, and the threat of misuse for bioterrorism, arenaviruses represent a serious health concern. LCMV is the prototypic member of the *arenaviridae* family, causing fatal illness in immunocompromised individuals and congenital brain malformation associated with mental retardation in infants (Barton et al., 2002; Peters, 2006). Like other arenaviruses, LCMV is a non-lytic enveloped virus with two negative stranded RNA segments (Meyer et al., 2002). The Small segment encodes the viral nucleoprotein (NP) and glycoprotein (GP) precursors, while the Large segment encodes the RNA-dependent RNA polymerase (L) and the matrix protein (Z). The surface of LCMV displays evenly distributed GP heterotrimers that bind to the cellular receptor α -dystroglycan (α -DG), which is shared by all Old-world arenaviruses, including the highly pathogenic Lassa virus (LASV) (Rojek and Kunz, 2008).

Among LCMV variants, LCMV clone 13 (C113) is of particular interest as it out-competes the ensuing immune response, resulting in chronic infection (Ahmed et al., 1984). Therefore, LCMV C113 has served as a model for both arenaviruses that outpace the human immune system, such as LASV, and for viruses that establish chronic infections such as HIV, HCV and HBV (Oldstone, 2007; Zinkernagel, 2002). The ability of LCMV C113 to outcompete its host has been related to a F>L mutation at position 260 of the GP, which enhances its binding affinity to α -DG and infection of target cells such as DCs, macrophages and fibroreticular cells, and a K>Q mutation at position 1079 of the viral polymerase that increases viral replicative capacity (Bergthaler et al., 2010; Matloubian et al., 1993; Mueller et al., 2007; Sullivan et al., 2011).

In the present study we investigated early pDC responses upon *in vivo* infection with LCMV C113. We found that, consistent with their capacity to preferentially bind to LCMV C113 and LASV GP, pDCs became rapidly infected with LCMV C113 to a higher degree than other leukocytes and were powerful producers of both IFN-I and IL-12. Intrinsic virus replication was not a requisite for pDC IFN-I production as uninfected (rather than infected) pDCs were numerically a greater source of IFN-I. Instead, pDC responses were globally mediated by TLR7, which limited their viral loads and promoted early activation of innate and adaptive immune cells. Our study aids the understanding of diseases caused by the highly pathogenic arenaviruses and other viruses that productively target and replicate within DCs.

RESULTS

LCMV and LASV glycoprotein preferentially bound to pDCs

Among splenic leukocytes, DCs express the highest levels of functional α -DG, consistent with DCs being a major target of LCMV C113 and LASV (Baize et al., 2004; Sevilla et al., 2003). To further discern Old-world arenavirus tropism within the heterogeneous DC population, we assessed binding of LCMV C113 and a pseudo-viral particle that expressed LASV GP (LASV-GP) to proteins isolated from bone marrow (BM)-derived pDCs and cDCs generated in the presence of fms-like tyrosine kinase receptor-3 ligand (Flt3L) or granulocyte macrophage colony stimulating factor (GM-CSF) (Figure 1A). We observed that both LCMV C113 and LASV-GP bound to pDCs to a greater extent than GM-CSF and Flt3L-derived cDCs, which exhibited lower or undetectable binding, respectively (Figure 1B). pDCs also expressed higher levels of LCMV NP than cDCs from Flt3L cultures generated from BM of infected mice (Figure 1C). To confirm these findings, splenic pDCs and cDCs (CD8⁺ and CD11b⁺ cDCs) were FACS purified from uninfected mice as indicated in Figure 1D, and protein lysates were assessed for binding to LCMV C113 and recombinant LCMV expressing the GP of LASV (rLCMV-LASV GP) (Rojek et al., 2008) (Figure 1E). Similar to BM-pDCs, *ex vivo* splenic pDCs bound both LCMV C113 and rLCMV-LASV-GP to a higher level than CD8⁺ and CD11b⁺ cDC subsets. Altogether, these results indicated that pDCs expressed functional receptor/s and exhibited greater binding to Old-world arenavirus GPs than cDCs, suggesting that they could be preferential and important targets upon LCMV C113 and LASV exposure.

LCMV C113 productively infected pDCs early after *in vivo* exposure

To investigate the degree of pDC infection in relation to other leukocytes early after *in vivo* exposure with LCMV C113, we purified splenic pDCs, CD8⁺ and CD11b⁺ cDCs, macrophages, B and T cells at day 1 p.i.. We found that pDCs exhibited the highest degree of LCMV C113 infection compared to the aforementioned leukocytes, as indicated by elevated levels of LCMV *gp* and *np* RNA transcripts (Figure 2A and data not shown). We validated these findings by infecting WT mice with a recombinant LCMV C113 virus that encodes green fluorescence protein (r3LCMV C113-GFP) (Emonet et al., 2009) and analyzed GFP⁺ DCs at day 1 p.i. We observed that CD11c⁺CD11b^{low/neg}PDCA⁺ cells comprised the majority of GFP⁺ DCs (GFP⁺) while they represented about one third of the GFP⁻ DCs (GFP⁻) (Figure 2B). Of note, B220 expression was intermediate in this GFP⁺ population (data not shown). To examine productive viral infection in pDCs, we performed infectious center assays. pDCs released significantly higher numbers of infectious particles as compared to the other leukocyte populations (Figure 2C). Of note, at day 5 p.i., pDCs continued being productive targets of LCMV C113 but, at this latter stage, cDCs also showed similarly high levels of infection (Figure S1). These data indicated that LCMV C113 rapidly infected pDCs to a significantly higher extent than other splenic leukocytes analyzed in this study, establishing a productive viral life cycle *in vivo*.

pDCs were powerful IFN-I and IL-12 producers early after LCMV C113 infection

pDC IFN-I response is silenced by day 5 of LCMV C113 infection (Lee et al., 2009; Zuniga et al., 2008), but whether pDCs produced IFN-I early after infection with the pDC-tropic LCMV C113 remained unknown. Analysis of *Ifna* and *Ifn β* RNA in splenocytes, obtained at day 1 after LCMV C113 infection, revealed the highest levels of IFN-I transcript in pDCs (Figure 3A). Accordingly, IFN-I bioactivity was significantly elevated in culture supernatants of pDCs from LCMV C113 infected, compared to uninfected, mice (Figure 3B). To confirm and extend these findings, we infected IFN β ^{mob/mob} mice, which express yellow fluorescent protein (YFP) under the IFN β promoter (Scheu et al., 2008), with LCMV C113. We observed that pDCs were the most potent IFN β producing cells in spleen, BM,

peripheral (p) and mesenteric (m) lymph nodes (LN), as indicated by the highest percentages of YFP⁺ cells in pDCs among all leukocytes analyzed (Figure 3C and S2A). Consistently, ~80% of YFP⁺ cells exhibited a pDC phenotype (Figure S2B). pDCs also produced multiple cytokines (i.e. IL-12, TNF α , IL1 α) as well as chemokines (i.e. MCP1, MIP1 β and RANTES) in response to infection (Figure S2C). We further studied IL-12 and TNF α production by flow cytometry. We found that a substantial fraction of splenic pDCs synthesized IL-12, to levels above cDCs and macrophages, suggesting pDCs are a major producer of IL-12 at this early time point (Figure 3D and S2D), whereas CD11b⁺ cDCs outnumbered pDCs when total TNF α -producing cells were enumerated in the spleen (Figure 3D and S2D). Finally, to assess whether different pDC subsets were responsible for distinct cytokine secretion, we analyzed IL-12 and TNF α production in pDCs from IFN β ^{mob/mob} mice. We detected that ~30–45% of IFN β -producing pDCs were co-producing IL-12, while a minor or undetectable fraction of these dual producers were synthesizing TNF α (Figure 3E). Altogether, these data indicated that pDCs were powerful IFN-I producing cells in several lymphoid tissues, with a proportion of them simultaneously secreting pro-inflammatory cytokines early after *in vivo* LCMV C113 infection.

pDCs matured but remained poor antigen presenting cells after LCMV C113 infection

Because pDCs were productively infected and rapidly secreted immune activating cytokines, we investigated their antigen presenting capacity. pDCs significantly upregulated major histocompatibility complex (MHC) I, MHC II, CD86, programmed death ligand 1 (PDL1), and CD40 expression at day 1 after LCMV C113 infection in comparison to uninfected controls and infected macrophages, albeit to a lesser extent than cDCs (Figure 4A and Figure S3). Notably, YFP⁺ and YFP⁻ pDCs from LCMV C113-infected IFN β ^{mob/mob} mice exhibited similar upregulation of MHC II and CD86 (Figure 4B), suggesting different requirements for pDC IFN-I production and maturation. Next, we directly tested the ability of pDCs to prime naïve LCMV-specific T cells in comparison with other antigen presenting cells. In contrast to pDCs, cDCs from infected mice successfully induced T cell proliferation and cytokine production in both LCMV specific CD8⁺ (higher induction by CD8⁺cDC) and CD4⁺ (higher induction by CD11b⁺cDC) T cells (Figure 4C). No proliferation or cytokine production was induced by DCs from uninfected mice (data not shown). These results indicated that, unlike cDCs and despite upregulated maturation markers early after infection, pDCs remained weak antigen presenting cells to both naïve CD4⁺ and CD8⁺ T cells.

pDC IFN-I production and maturation were dissociated from intrinsic LCMV replication

Arenavirus NPs are powerful inhibitors of IFN-I production (Martinez-Sobrido et al., 2006). To test the effect of intrinsic LCMV replication on early pDC IFN-I production, we infected WT or IFN β ^{mob/mob} mice with r3LCMV C113-GFP or WT C113. The proportions of YFP⁺ or YFP⁻ pDCs and cDCs that were infected (GFP⁺) or uninfected (GFP⁻) were analyzed. A similar proportion of both GFP⁺ and GFP⁻ pDCs produced IFN β , although uninfected pDCs producing IFN β were more numerous (Figure 5A). In contrast, only infected (GFP⁺) cDCs appeared to be producing IFN β , suggesting that cDCs required intrinsic viral replication for IFN-I induction (Figure 5A and S). We confirmed IFN-I production in infected pDCs by injecting IFN β ^{mob/mob} mice with WT LCMV C113 followed by FACS purification of YFP⁺ and YFP⁻ pDCs. We observed that IFN β -YFP⁺ pDCs expressed higher transcript levels of LCMV *gp* and *np* (Figure 5B) and exhibited a tendency toward increased numbers of infectious viral particles produced per pDC when compared to YFP⁻ pDCs (Figure 5C). Lastly, we determined the localization of IFN β producing, as well as LCMV-infected, cells in the spleen, by immunofluorescence microscopy (Figure 5D). LCMV⁺ cells were located primarily bordering lymphoid follicles of the spleen, as previously reported (Borrow et al., 1995), and YFP⁺ cells were roughly within the same areas. In agreement with the above flow cytometric data, YFP⁺ signal was readily detected in both infected and uninfected cells

(Figure 5D). Altogether, these data provided *in vivo* evidence that pDCs do not require intrinsic viral replication to secrete IFN-I and that uninfected (rather than infected) pDCs were quantitatively the major source of IFN-I at the peak of its response. Notably, pDC IFN-I production was not completely inhibited by intrinsic LCMV replication but the majority of infected pDCs (and cDCs) did not induce IFN-I in response to the intrinsically replicating virus.

TLR7 was essential for early pDC response after LCMV CI13 infection

A previous study proposed that pDCs may use a MyD88-dependent TLR7 and TLR9-partially-independent pathway to sense LCMV *in vivo* (Jung et al., 2008) while another study demonstrated that pDCs produce IFN-I in response to transfected LCMV RNA in a MyD88-independent manner (Zhou et al., 2010). To shed light on this issue, we investigated systemic and pDC-derived IFN-I production in WT versus TLR7^{-/-} LCMV-CI13-infected mice at day 1 p.i. TLR7^{-/-} mice exhibited significantly reduced levels of serum IFN-I, although substantial levels were still detected (Figure 6A). In contrast, *Ifna* and *Ifnβ* RNA expression in pDCs and IFN-I bioactivity in pDC culture supernatants were completely ablated in the absence of TLR7 (Figure 6B–C). Only background levels of *Ifna* and *Ifnβ* transcript were detected in cDCs and macrophages from both WT and TLR7^{-/-} infected mice. Similarly, IL-12 levels were significantly decreased in pDC culture supernatants and flow cytometric analysis in TLR7^{-/-} compared to WT infected mice (Figure 6D & 6E). We also observed that the TLR7^{-/-} pDCs exhibited significantly lower levels of MHC II, CD86, and PDL1 compared to WT infected mice (Figure 6F). Finally, we investigated viral loads in pDCs from WT and TLR7^{-/-} mice at day 1 p.i. We found that pDCs from TLR7^{-/-} infected mice had enhanced levels of LCMV *gp* and *np* transcripts in comparison to WT controls (Figure 6G). These findings demonstrated that TLR7 played a central role in pDC recognition of LCMV, mediating rapid pDC maturation and production of IFN-I and IL-12, as well as limiting viral replication within pDCs early after *in vivo* infection.

TLR7 was required for full activation of innate and adaptive immune cells early after LCMV CI13 infection

We next investigated the activation status of other innate (cDCs and NK cells) as well as adaptive (CD4⁺ and CD8⁺ T cells) immune cells in TLR7^{-/-} and WT infected mice. In contrast to pDCs, the numbers of IL-12 and TNFα producing cDCs and macrophages were not affected, or were slightly increased, by TLR7 deficiency (Figure 7A). However, we observed that both TLR7^{-/-} cDCs and macrophages exhibited lower expression of MHCII, CD86, and PDL1 compared with their WT counterparts, although these cells were still more matured compared to uninfected controls (Figure 7B–D). Similarly, expression of the early activation marker CD69 was significantly upregulated in NK, CD4⁺ and CD8⁺ T cells from WT infected *versus* uninfected mice, but its expression was compromised in TLR7^{-/-} infected mice (Figure 7E). Overall, these results indicated that TLR7 exerted a global effect in orchestrating innate and adaptive immune cells early after LCMV CI13 infection.

DISCUSSION

It is well established that the initial interactions between a pathogen and its host can drastically influence the outcome of an infection. We characterized the early events that unfold upon *in vivo* exposure with a prototypic member of the family *Arenaviridae*, which includes causative agents of fatal hemorrhagic fevers, as well as established models for studying antiviral immunity. Our data unveiled pDCs as an early target for productive arenavirus replication, situating this cell type at the center of the virus-host battle during the onset of an *in vivo* infection.

DCs express high levels of functional α -DG and have been defined as major targets of Old-world arenaviruses in mice and humans, an event related to DC functional impairment and T cell suppression (Baize et al., 2004; Pannetier et al., 2011; Sevilla et al., 2003). More recently, using infection of GFP reporter transgenic mice with a replication deficient LCMV vector, GFP expression was exclusively detected in DCs, particularly PDCA⁺CD11c^{int} cells (Bergthaler et al., 2010). This observation suggests that pDCs are the initial targets of LCMV but it remained open whether pDCs could support a productive viral cycle. By using a stringent pDC purification protocol coupled with infectious center assay, we demonstrated that, as early as 1 day after *in vivo* exposure with LCMV C113, pDCs produced significantly more infectious viral particles than any other leukocyte analyzed in this study, suggesting their potential role in initial viral propagation. Our data also showed that pDCs expressed higher levels of Old-world arenavirus-binding proteins than cDCs, providing an explanation for why pDCs are preferentially targeted by LCMV C113 (and possibly LASV) *in vivo*.

IFN-I plays a crucial role in virus control and induction of virus-specific T cells in several infections including those with single stranded (ss) RNA viruses such as LCMV (Muller et al., 1994; van den Broek et al., 1995), influenza virus (Wiesel et al., 2011), HCV (Missale et al., 1997; Rodrigue-Gervais et al., 2010), and HIV (Meyers et al., 2007). Consistently, a complex and often overlapping molecular network is in place to secure rapid viral sensing and IFN-I production. In particular, ssRNA viruses can trigger IFN-I production mainly through the cytoplasmic RIG-I/MAVS/IRF3 pathway and the endosomal TLR7/MyD88/IRF7 pathway, the latter operating exclusively in pDCs (Thompson et al., 2011). However, most viruses have evolved strategies to counteract IFN-I production and signaling to favor their own replication and transmission (Garcia-Sastre and Biron, 2006). Thus, a common query for many viral infections is how IFN-I is elevated *in vivo* despite the inhibitory activity of viral products. In that regard, NPs from most arenaviruses inhibit IFN-I production (Martinez-Sobrido et al., 2007) but IFN-I is still elevated early after infection (Lee et al., 2009; Louten et al., 2006; Zuniga et al., 2008). Several studies have attributed the cellular source of IFN-I during LCMV infection to marginal zone macrophages (Louten et al., 2006), cDCs, and pDCs (Dalod et al., 2002; Diebold et al., 2003; Jung et al., 2008; Lee et al., 2009; Montoya et al., 2005; Zhou et al., 2010) under conditions that result in acute viral clearance. We found pDCs were a powerful early source of IFN-I in several lymphoid tissues after infection with DC-tropic LCMV C113, which establishes chronic infection (Ahmed et al., 1984). Remarkably, and in contrast to cDCs, pDCs did not require intrinsic LCMV replication to produce IFN-I, and, indeed, uninfected pDCs were quantitatively a major leukocyte source of IFN-I, supporting previous data demonstrating IFN-I production by uninfected pDCs during infection with murine cytomegalovirus (MCMV) (Dalod et al., 2003) or Newcastle Disease virus (Kumagai et al., 2009). On the other hand, a fraction of infected pDCs (and cDCs) also produced IFN-I but the vast majority did not, possibly due to the inhibitory effect of the arenavirus NP (Martinez-Sobrido et al., 2006). These data suggest that pDCs may have evolved means to sense virus infection independent of intrinsic replication. In this regard, a cell-to-cell RNA transfer process during which HCV-infected cells induce pDC IFN-I production, without infecting them, has been reported (Takahashi et al., 2010). To date, the TLRs involved in sensing LCMV to initiate *in vivo* IFN-I production remain controversial. TLR2ko mice, but not 3D mice which exhibit impaired TLR3, TLR7 and TLR9 responses, showed reduced IFN-I upregulation upon *in vivo* infection with LCMV (Zhou et al., 2005). In contrast, another study reported that IFN-I response was partially inhibited in TLR7 and TLR9 double ko mice (but not TLR2ko mice) and proposed that pDCs recognize LCMV partially through an unknown receptor that signals through MyD88 (Jung et al., 2008). Our data clearly indicated that TLR7 was absolutely essential for pDC IFN-I production and partially required for systemic IFN-I elevation after *in vivo* LCMV C113 infection. Indeed, while pDC IFN-I was completely ablated in TLR7^{-/-} infected mice, substantial amounts of systemic IFN-I were still detected, indicating that

other cell types significantly contribute to systemic IFN-I elevation early after *in vivo* infection, as previously reported (Dalod et al., 2002; Louten et al., 2006; Swiecki et al., 2010).

Not only were pDCs able to produce substantial levels of IFN-I, but they also secreted multiple other cytokines and chemokines in response to *in vivo* LCMV CI13 infection. In particular, IL-12 was mainly secreted by pDCs in a TLR7-dependent fashion. This is in agreement with previous studies in MCMV infection that demonstrated pDCs are a major source of both IFN-I and IL-12, although the source of IL-12 (but not IFN-I) can be substituted by other DC subsets (Dalod et al., 2003; Dalod et al., 2002; Krug et al., 2004). Here we observed that a proportion of IFN-I producing pDCs simultaneously synthesized IL-12, and to a lower extent TNF α , uncovering multi-cytokine producing pDCs that arise early after *in vivo* LCMV CI13 infection, as has been observed after MCMV infection (Zucchini et al., 2008). Furthermore, while CD11b⁺cDCs and CD8⁺cDCs exhibited strong antigen presenting capacity early after LCMV CI13 infection, pDCs remained poor antigen presenting cells. The preferential antigen presentation of CD8⁺cDCs to CD8⁺T cells and CD11b⁺cDCs to CD4⁺T cells is in agreement with previous work demonstrating that these cDC subsets are equipped to better present MHC I or II antigens, respectively (Dudziak et al., 2007). pDCs may instead play an indirect role in the initial activation of innate and adaptive immune cells through IL-12 and IFN-I production. Although we did not directly link pDC cytokine production with the early activation of immune cells during LCMV CI13 infection, the well established role of both IL-12 and IFN-I in this process (Biron et al., 2002; Swiecki and Colonna, 2011), as well as the diminished activation of cDCs, NK cells and T cells that we observed in TLR7^{-/-} mice support this possibility. In this regard, a recent study demonstrates that pDC depletion by conditional targeting of the E2-2 transcription factor results in impaired antiviral T cell responses and failure to control persistent LCMV Docile infection (Cervantes-Barragan et al., 2012). On the other hand, another report shows that pDC depletion in BDCA2-DTR transgenic mice infected with persistent LCMV CI13 causes no effect on CD8 T cell responses and only slight increases in viral load at 48 hr p.i. (Wang et al CH&M 2012). Nonetheless, we and others demonstrated that pDC numbers and their IFN-I production capacity are severely reduced by day 5 after LCMV CI13 infection (Lee et al., 2009; Zuniga et al., 2008), suggesting that understanding the mechanisms involved in pDC suppression may illuminate strategies to prolong pDC-derived IFN-I responses and promote a more potent antiviral response. Finally, our results indicated that TLR7 signaling limited viral loads in pDCs at a time when they were a niche for productive infection. These findings were consistent with previous reports demonstrating that TLR7 controls immune responses during infection with other ssRNA viruses (Diebold et al., 2003; Hornung et al., 2005; Lund et al., 2004; Schlaepfer et al., 2006). Furthermore, another study shows that TLR7^{-/-} mice fail to control viremia due to multiple defects in the adaptive immune response during chronic LCMV infection (Walsh et al CH&M June 2012). This study, together with our results, points to the TLR7 pathway as a potential target to improve control of Old-world arenaviruses.

Our study uncovered pDCs as a preferential leukocyte target for productive virus replication and a powerful source of antiviral and pro-inflammatory cytokines during *in vivo* infection with a prototypic Old-world arenavirus. This situates the pDC as a double-edged sword in the virus-host competition that takes place early (and that may influence later events) during infection with arenaviruses and potentially other DC-tropic viruses.

EXPERIMENTAL PROCEDURES

Mice and viral stocks

WT C57Bl/6 and IFN β ^{mob/mob} mice were purchased from The Jackson Laboratory (Bar Harbor, Maine). TLR7^{-/-} mice were described previously (Lund et al., 2004). Mice were bred and maintained in a closed breeding facility and mouse handling complied with the requirements of the National Institutes of Health and the Institutional Animal Care and Use Guidelines of the University of California San Diego. 6–10 week old mice were infected intravenously with 2×10^6 pfu/mL WT LCMV Cl13 or LCMV Armstrong 53b (ARM), or 4.5×10^5 pfu/mL r3LCMVC113-GFP (Emonet et al., 2009). All viruses were grown, identified, and quantified as previously described (de la Torre and Oldstone, 1992).

Cell Purification

Spleens were incubated with collagenase D (1mg/mL, Roche, Indianapolis, IN) for 20 min at 37°C and passed through a 100 μ m strainer to achieve a single cell suspension. Splenocytes were enriched with PanDC or PDCA microbeads using an Automacs system (Miltenyi, Auburn, CA). PanDC⁺ fractions were FACS-purified using a BD ARIA (BD Biosciences, San Jose, CA) for pDCs (CD11c^{intermediate/dim}CD11b⁻B220⁺PDCA⁺), CD8⁺ cDCs (CD11c⁺B220⁻CD11b⁻CD8⁺) and CD11b⁺ cDCs (CD11c⁺B220⁻CD11b⁺CD8⁻) after B (CD19), T (Thy1.2) and NK (Nk1.1) cell exclusion. PanDC⁻ fractions were FACS-purified for macrophages (CD19⁻Thy1.2⁻NK1.1⁻CD11c⁻CD11b⁺) and B/T cells (Thy1.2⁺CD19⁺). WT Cl13 infected IFN β ^{mob/mob} pDCs were FACS-purified for IFN β producing (pDC YFP⁺) and non-producing (pDC YFP⁻) cells. Purity for all cell types was >94%.

Flow cytometry

Antibodies used were purchased from Ebioscience or BD Pharmingen (San Diego, CA) to stain splenocytes: CD19 PE, efluor450, or PercpCy5.5, Thy1.2 PE, efluor450, or PercpCy5.5, NK1.1 PE, efluor450, or PercpCy5.5, CD11c APC or Alexa700, PDCA1 FITC or PE, CD11b PercpCy5.5, PECy7, or APC, B220 APC-efluor780, IL-12p40 Alexa647, and TNF α efluor450. Cells were preincubated with CD16/CD32 Fc block (BD Pharmingen). Anti-LCMV-NP (clone 113) was a gift from M Oldstone (TSRI). Surface and intracellular cytokine staining was performed as previously described (Zuniga et al., 2004). Samples were acquired on a BD LSR II (BD biosciences) and analyzed using FlowJo software (Treestar, Inc., Ashland, OR).

Virus Overlay Assay

pDCs and cDCs were generated from BM cells in the presence of fms-like tyrosine kinase receptor-3 ligand (Flt3L; 100 ng/ml) or GM-CSF (200 IU) as previously described (Zuniga et al., 2004). For virus overlay assay, proteins were separated by SDS-PAGE, blotted to nitrocellulose and incubated with purified LCMV Cl13 and VSV pseudoparticles expressing LASV GP at 10^7 PFU/ml. Bound virus was detected with mAb 83.6 to LCMV GP2 using an HRP-conjugated secondary antibody and ECL for detection as described (Kunz et al., 2005).

Virus Binding Assay

3×10^5 cells (pDCs, CD8⁺ cDCs, and CD11b⁺ cDCs) were lysed in 50 mM Hepes pH 7.5/150mM NaCl/1% NP-40/1.2mM EDTA/5mM MgCl₂, 5mM CaCl₂/protease inhibitor cocktail complete (Roche), and 1 mM PMSF. Lysates were cleared and subjected to affinity purification with wheat germ agglutinin (WGA) as described (Michele et al., 2002). Eluted glycoproteins were immobilized in 96-well microtiter (EIA/RIA) high-bond plates and non-specific binding was blocked with 1% (w/v) BSA/PBS 1hr at room temperature (RT).

LCMV Cl13 and recombinant LCMV expressing the GP of LASV (Rojek et al., 2008) were purified over a renografin gradient and diluted in 1% (w/v) BSA/PBS to 10^7 PFU/ml. Virus was incubated overnight (O/N) on a shaker, unbound virus removed by washing, and bound virus detected with mAb 83.6 to LCMV GP2 with a biotinylated secondary antibody and streptavidin-HRP in a color reaction with 2,2'-azino-bis(3-ethylbenzthiazoline-6-sulfonic acid (ABTS). Jurkat cells, which are negative for LASV receptors and refractory to infection, were used as negative controls.

Antigen Presentation Assay

2.5×10^4 FACS-purified DCs were co-cultured with 5×10^4 naïve CFSE labeled TCR transgenic P14⁺ or SMARTA⁺T cells enriched to >90% by negative selection (Stem Cell Technology, Vancouver, Canada). 72 hrs later, T cells were re-stimulated with cognate peptide GP₃₃₋₄₁ (P14) or GP₆₇₋₇₇ (SMARTA) for 5 hrs in the presence of brefeldin A (BFA) and analyzed for CFSE dilution and intracellular cytokine production of IFN γ , TNF α , and IL-2 by flow cytometry (BD LSRII).

Immunofluorescence

Snap frozen OCT embedded spleens from WT Cl13 infected IFN β ^{mob/mob} mice were cut into 6 μ m sections using a cryostat (Leica, Buffalo Grove, IL) and mounted onto glass slides. Sections were fixed by 4% paraformaldehyde RT 15min, permeabilized with 0.2% NP40 in 1x PBS+5% BSA 5 min RT, blocked 30 min RT with image iT Fx signal enhancer (Invitrogen, Carlsbad, CA), and incubated O/N at 4°C with guinea pig anti-LCMV (1:200) and rabbit anti-GFP antibodies (1:100, Cell Signaling, Danvers, MA). Rhodamine RedX conjugated donkey anti-guinea pig (1:200, Jackson ImmunoResearch, Westgrove, PA) and FITC conjugated anti-rabbit Ig (1:50, eBioscience) secondary antibodies were incubated with sections for 1 hr. Nuclei were stained with DAPI (1:1000, Sigma Aldrich, St. Louis, MO) 5 min RT prior to mounting. Sections were imaged at 100x magnification on an Olympus FV1000 Confocal Microscope and analyzed using FV10-ASW v3.0 viewer software.

Infectious Center Assay

Two-fold dilutions of FACS-purified splenocytes were prepared and incubated on a Vero cell monolayer with rotation for 1hr at 37°C. Monolayers were then overlaid with 1% agarose and incubated 6 days at 37°C. Release of viral progeny determined as plaques formed was quantified and extrapolated as number of plaques per million cells as described previously (Doyle and Oldstone, 1978).

Cytokine Measurements

For cytokine measurement in culture supernatants, 50,000 FACS-purified pDCs were cultured for 15hrs at 37°C. IFN-I bioactivity was measured with reference to a recombinant mouse IFN β standard (Research Diagnostics, Concord, MA) using a L-929 cell line transfected with an interferon-sensitive luciferase (Jiang et al., 2005). IL-12p70, TNF α , IL-1 α , MCP1, MIP1 α , and RANTES were measured in culture supernatants by luminex array using readymade MILLIPLEX mouse cytokine panel I and II kits (Millipore, Billerica, MA) as described previously (Harker et al., 2011). To measure intracellular cytokines by flow cytometry, splenocytes were incubated in complete media + BFA for 4hrs at 37°C prior to staining.

Quantitative Real-time RT-PCR analysis

Total RNA was extracted from purified cells using RNeasy Microkit (Qiagen, Valencia, CA), digested with DNase I and reverse transcribed into cDNA (Superscript III, Invitrogen,

Carlsbad, CA). Quantification of cDNA was performed using SYBR Green PCR Kit and Real-Time PCR Detection System (Applied Biosystem, Carlsbad, CA). The relative RNA levels were normalized against GAPDH RNA as described previously (Zuniga et al., 2008). The following primers were used: LCMV glycoprotein: F 5'-CATTACCTGGACTTTGTCAGACTC-3' R 5'-GCAACTGCTGTGTTCCCCGAAA-3'; LCMV nucleoprotein: F 5'-GCATTGTCTGGCTGTAGCTTA-3'; R 5'-CAATGACGTTGTACAAGCGC-3'; IFN α 4: F 5'-TATGTCCTCACAGCCAGCAG-3' R 5'-TTCTGCAATGACCTCCATCA-3'; IFN β : F 5'-CTGG CTTCCATCATGAACAA-3' R 5'-AGAGGGCTGTGGTGGAGAA-3.

Statistical Analysis

Statistical differences were determined by one way or two way analysis of variance (ANOVA) or student's T-test using the InStat 3.0 software (Graphpad, La Jolla, CA).

Supplementary Material

Refer to Web version on PubMed Central for supplementary material.

Acknowledgments

We thank Dr. J.C. de la Torre for generously providing r3LCMVC113-GFP and Aaron Chang for technical assistance. This study was supported by grants from the National Institute of Health A1081923 to EZ and A1081923 supplement to MM.

References

- Ahmed R, Salmi A, Butler LD, Chiller JM, Oldstone MB. Selection of genetic variants of lymphocytic choriomeningitis virus in spleens of persistently infected mice. Role in suppression of cytotoxic T lymphocyte response and viral persistence. *J Exp Med*. 1984; 160:521–540. [PubMed: 6332167]
- Baize S, Kaplon J, Faure C, Pannetier D, Georges-Courbot MC, Deubel V. Lassa virus infection of human dendritic cells and macrophages is productive but fails to activate cells. *J Immunol*. 2004; 172:2861–2869. [PubMed: 14978087]
- Banchereau J, Steinman RM. Dendritic cells and the control of immunity. *Nature*. 1998; 392:245–252. [PubMed: 9521319]
- Barton LL, Mets MB, Beauchamp CL. Lymphocytic choriomeningitis virus: emerging fetal teratogen. *Am J Obstet Gynecol*. 2002; 187:1715–1716. [PubMed: 12501090]
- Bergthaler A, Flatz L, Hegazy AN, Johnson S, Horvath E, Lohning M, Pinschewer DD. Viral replicative capacity is the primary determinant of lymphocytic choriomeningitis virus persistence and immunosuppression. *Proc Natl Acad Sci U S A*. 2010; 107:21641–21646. [PubMed: 21098292]
- Biron CA, Nguyen KB, Pien GC. Innate immune responses to LCMV infections: natural killer cells and cytokines. *Curr Top Microbiol Immunol*. 2002; 263:7–27. [PubMed: 11987821]
- Borrow P, Evans CF, Oldstone MB. Virus-induced immunosuppression: immune system-mediated destruction of virus-infected dendritic cells results in generalized immune suppression. *J Virol*. 1995; 69:1059–1070. [PubMed: 7815484]
- Cervantes-Barragan L, Lewis KL, Firner S, Thiel V, Hugues S, Reith W, Ludewig B, Reizis B. Plasmacytoid dendritic cells control T-cell response to chronic viral infection. *Proc Natl Acad Sci U S A*. 2012
- Cousens LP, Orange JS, Su HC, Biron CA. Interferon-alpha/beta inhibition of interleukin 12 and interferon-gamma production in vitro and endogenously during viral infection. *Proc Natl Acad Sci U S A*. 1997; 94:634–639. [PubMed: 9012836]
- Dalod M, Hamilton T, Salomon R, Salazar-Mather TP, Henry SC, Hamilton JD, Biron CA. Dendritic cell responses to early murine cytomegalovirus infection: subset functional specialization and differential regulation by interferon alpha/beta. *J Exp Med*. 2003; 197:885–898. [PubMed: 12682109]

- Dalod M, Salazar-Mather TP, Malmgaard L, Lewis C, Asselin-Paturel C, Briere F, Trinchieri G, Biron CA. Interferon alpha/beta and interleukin 12 responses to viral infections: pathways regulating dendritic cell cytokine expression in vivo. *J Exp Med*. 2002; 195:517–528. [PubMed: 11854364]
- de la Torre JC, Oldstone MB. Selective disruption of growth hormone transcription machinery by viral infection. *Proc Natl Acad Sci U S A*. 1992; 89:9939–9943. [PubMed: 1409723]
- Diebold SS, Montoya M, Unger H, Alexopoulou L, Roy P, Haswell LE, Al-Shamkhani A, Flavell R, Borrow P, Reis e Sousa C. Viral infection switches non-plasmacytoid dendritic cells into high interferon producers. *Nature*. 2003; 424:324–328. [PubMed: 12819664]
- Doyle MV, Oldstone MB. Interactions between viruses and lymphocytes. I. In vivo replication of lymphocytic choriomeningitis virus in mononuclear cells during both chronic and acute viral infections. *J Immunol*. 1978; 121:1262–1269. [PubMed: 308960]
- Dudziak D, Kamphorst AO, Heidkamp GF, Buchholz VR, Trumfheller C, Yamazaki S, Cheong C, Liu K, Lee HW, Park CG, et al. Differential antigen processing by dendritic cell subsets in vivo. *Science*. 2007; 315:107–111. [PubMed: 17204652]
- Emonet SF, Garidou L, McGavern DB, de la Torre JC. Generation of recombinant lymphocytic choriomeningitis viruses with trisegmented genomes stably expressing two additional genes of interest. *Proc Natl Acad Sci U S A*. 2009; 106:3473–3478. [PubMed: 19208813]
- Fitzgerald-Bocarsly P, Jacobs ES. Plasmacytoid dendritic cells in HIV infection: striking a delicate balance. *J Leukoc Biol*. 2010; 87:609–620. [PubMed: 20145197]
- Garcia-Sastre A, Biron CA. Type 1 interferons and the virus-host relationship: a lesson in detente. *Science*. 2006; 312:879–882. [PubMed: 16690858]
- Geisbert TW, Jahrling PB. Exotic emerging viral diseases: progress and challenges. *Nat Med*. 2004; 10:S110–121. [PubMed: 15577929]
- Harker JA, Lewis GM, Mack L, Zuniga EI. Late interleukin-6 escalates T follicular helper cell responses and controls a chronic viral infection. *Science*. 2011; 334:825–829. [PubMed: 21960530]
- Hornung V, Guenther-Biller M, Bourquin C, Ablasser A, Schlee M, Uematsu S, Noronha A, Manoharan M, Akira S, de Fougerolles A, et al. Sequence-specific potent induction of IFN- α by short interfering RNA in plasmacytoid dendritic cells through TLR7. *Nat Med*. 2005; 11:263–270. [PubMed: 15723075]
- Jiang Z, Georgel P, Du X, Shamel L, Sovath S, Mudd S, Huber M, Kalis C, Keck S, Galanos C, et al. CD14 is required for MyD88-independent LPS signaling. *Nat Immunol*. 2005; 6:565–570. [PubMed: 15895089]
- Jung A, Kato H, Kumagai Y, Kumar H, Kawai T, Takeuchi O, Akira S. Lymphocytoid choriomeningitis virus activates plasmacytoid dendritic cells and induces a cytotoxic T-cell response via MyD88. *J Virol*. 2008; 82:196–206. [PubMed: 17942529]
- Krug A, French AR, Barchet W, Fischer JA, Dzionek A, Pingel JT, Orihuela MM, Akira S, Yokoyama WM, Colonna M. TLR9-dependent recognition of MCMV by IPC and DC generates coordinated cytokine responses that activate antiviral NK cell function. *Immunity*. 2004; 21:107–119. [PubMed: 15345224]
- Kumagai Y, Kumar H, Koyama S, Kawai T, Takeuchi O, Akira S. Cutting Edge: TLR-Dependent viral recognition along with type I IFN positive feedback signaling masks the requirement of viral replication for IFN- α production in plasmacytoid dendritic cells. *J Immunol*. 2009; 182:3960–3964. [PubMed: 19299691]
- Kunz S, Rojek J, Spiropoulou C, Barresi R, Campbell KP, MBO. Post-translational modification of alpha-dystroglycan, the cellular receptor for arenaviruses by the glycosyltransferase LARGE is critical for virus binding. *J Virol*. 2005; 79:14282–14296. [PubMed: 16254363]
- Lee LN, Burke S, Montoya M, Borrow P. Multiple mechanisms contribute to impairment of type 1 interferon production during chronic lymphocytic choriomeningitis virus infection of mice. *J Immunol*. 2009; 182:7178–7189. [PubMed: 19454715]
- Louten J, van Rooijen N, Biron CA. Type 1 IFN deficiency in the absence of normal splenic architecture during lymphocytic choriomeningitis virus infection. *J Immunol*. 2006; 177:3266–3272. [PubMed: 16920967]

- Lund JM, Alexopoulou L, Sato A, Karow M, Adams NC, Gale NW, Iwasaki A, Flavell RA. Recognition of single-stranded RNA viruses by Toll-like receptor 7. *Proc Natl Acad Sci U S A*. 2004; 101:5598–5603. [PubMed: 15034168]
- Martinez-Sobrido L, Giannakas P, Cubitt B, Garcia-Sastre A, de la Torre JC. Differential inhibition of type I interferon induction by arenavirus nucleoproteins. *J Virol*. 2007; 81:12696–12703. [PubMed: 17804508]
- Martinez-Sobrido L, Zuniga EI, Rosario D, Garcia-Sastre A, de la Torre JC. Inhibition of the type I interferon response by the nucleoprotein of the prototypic arenavirus lymphocytic choriomeningitis virus. *J Virol*. 2006; 80:9192–9199. [PubMed: 16940530]
- Matloubian M, Kolhekar SR, Somasundaram T, Ahmed R. Molecular determinants of macrophage tropism and viral persistence: importance of single amino acid changes in the polymerase and glycoprotein of lymphocytic choriomeningitis virus. *J Virol*. 1993; 67:7340–7349. [PubMed: 7693969]
- McCormick JB, Fisher-Hoch SP. Lassa fever. *Curr Top Microbiol Immunol*. 2002; 262:75–109. [PubMed: 11987809]
- McRae BL, Semnani RT, Hayes MP, van Seventer GA. Type I IFNs inhibit human dendritic cell IL-12 production and Th1 cell development. *J Immunol*. 1998; 160:4298–4304. [PubMed: 9574532]
- Meyer BJ, de la Torre JC, Southern PJ. Arenaviruses: genomic RNAs, transcription, and replication. *Curr Top Microbiol Immunol*. 2002; 262:139–157. [PubMed: 11987804]
- Meyers JH, Justement JS, Hallahan CW, Blair ET, Sun YA, O’Shea MA, Roby G, Kottlilil S, Moir S, Kovacs CM, et al. Impact of HIV on cell survival and antiviral activity of plasmacytoid dendritic cells. *PLoS One*. 2007; 2:e458. [PubMed: 17520017]
- Michele DE, Barresi R, Kanagawa M, Saito F, Cohn RD, Satz JS, Dollar J, Nishino I, Kelley RI, Somer H, et al. Post-translational disruption of dystroglycan-ligand interactions in congenital muscular dystrophies. *Nature*. 2002; 418:417–422. [PubMed: 12140558]
- Missale G, Cariani E, Lamonaca V, Ravaggi A, Rossini A, Bertoni R, Houghton M, Matsuura Y, Miyamura T, Fiaccadori F, et al. Effects of interferon treatment on the antiviral T-cell response in hepatitis C virus genotype 1b- and genotype 2c-infected patients. *Hepatology*. 1997; 26:792–797. [PubMed: 9303515]
- Montoya M, Edwards MJ, Reid DM, Borrow P. Rapid activation of spleen dendritic cell subsets following lymphocytic choriomeningitis virus infection of mice: analysis of the involvement of type I IFN. *J Immunol*. 2005; 174:1851–1861. [PubMed: 15699111]
- Mueller SN, Matloubian M, Clemens DM, Sharpe AH, Freeman GJ, Gangappa S, Larsen CP, Ahmed R. Viral targeting of fibroblastic reticular cells contributes to immunosuppression and persistence during chronic infection. *Proc Natl Acad Sci U S A*. 2007; 104:15430–15435. [PubMed: 17878315]
- Muller U, Steinhoff U, Reis LF, Hemmi S, Pavlovic J, Zinkernagel RM, Aguet M. Functional role of type I and type II interferons in antiviral defense. *Science*. 1994; 264:1918–1921. [PubMed: 8009221]
- Oldstone MB. Arenaviruses. I. The epidemiology molecular and cell biology of arenaviruses. Introduction *Curr Top Microbiol Immunol*. 2002; 262:V–XII.
- Oldstone MB. A suspenseful game of ‘hide and seek’ between virus and host. *Nat Immunol*. 2007; 8:325–327. [PubMed: 17375090]
- Pannetier D, Reynard S, Russier M, Journeaux A, Tordo N, Deubel V, Baize S. Human dendritic cells infected with the nonpathogenic Mopeia virus induce stronger T-cell responses than those infected with Lassa virus. *J Virol*. 2011; 85:8293–8306. [PubMed: 21632749]
- Peters CJ. Lymphocytic choriomeningitis virus—an old enemy up to new tricks. *N Engl J Med*. 2006; 354:2208–2211. [PubMed: 16723613]
- Reizis B, Bunin A, Ghosh HS, Lewis KL, Sisirak V. Plasmacytoid dendritic cells: recent progress and open questions. *Annu Rev Immunol*. 2011; 29:163–183. [PubMed: 21219184]
- Rodrigue-Gervais IG, Rigsby H, Jouan L, Sauve D, Sekaly RP, Willems B, Lamarre D. Dendritic cell inhibition is connected to exhaustion of CD8+ T cell polyfunctionality during chronic hepatitis C virus infection. *J Immunol*. 2010; 184:3134–3144. [PubMed: 20173023]

- Rojek JM, Kunz S. Cell entry by human pathogenic arenaviruses. *Cell Microbiol.* 2008; 10:828–835. [PubMed: 18182084]
- Rojek JM, Sanchez AB, Nguyen NT, de la Torre JC, Kunz S. Different mechanisms of cell entry by human-pathogenic Old World and New World arenaviruses. *J Virol.* 2008; 82:7677–7687. [PubMed: 18508885]
- Scheu S, Dresing P, Locksley RM. Visualization of IFN β production by plasmacytoid versus conventional dendritic cells under specific stimulation conditions in vivo. *Proc Natl Acad Sci U S A.* 2008; 105:20416–20421. [PubMed: 19088190]
- Schlaepfer E, Audige A, Joller H, Speck RF. TLR7/8 triggering exerts opposing effects in acute versus latent HIV infection. *J Immunol.* 2006; 176:2888–2895. [PubMed: 16493046]
- Sevilla N, Kunz S, McGavern D, Oldstone MB. Infection of dendritic cells by lymphocytic choriomeningitis virus. *Curr Top Microbiol Immunol.* 2003; 276:125–144. [PubMed: 12797446]
- Shortman K. Burnet oration: dendritic cells: multiple subtypes, multiple origins, multiple functions. *Immunol Cell Biol.* 2000; 78:161–165. [PubMed: 10762417]
- Sullivan BM, Emonet SF, Welch MJ, Lee AM, Campbell KP, de la Torre JC, Oldstone MB. Point mutation in the glycoprotein of lymphocytic choriomeningitis virus is necessary for receptor binding, dendritic cell infection, and long-term persistence. *Proc Natl Acad Sci U S A.* 2011; 108:2969–2974. [PubMed: 21270335]
- Swiecki M, Colonna M. Unraveling the functions of plasmacytoid dendritic cells during viral infections, autoimmunity, and tolerance. *Immunol Rev.* 234:142–162. [PubMed: 20193017]
- Swiecki M, Colonna M. Type I interferons: diversity of sources, production pathways and effects on immune responses. *Current Opinion in Virology.* 2011; 1:463–475. [PubMed: 22440910]
- Swiecki M, Gilfillan S, Vermi W, Wang Y, Colonna M. Plasmacytoid dendritic cell ablation impacts early interferon responses and antiviral NK and CD8(+) T cell accrual. *Immunity.* 2010; 33:955–966. [PubMed: 21130004]
- Takahashi K, Asabe S, Wieland S, Garaigorta U, Gastaminza P, Isogawa M, Chisari FV. Plasmacytoid dendritic cells sense hepatitis C virus-infected cells, produce interferon, and inhibit infection. *Proc Natl Acad Sci U S A.* 2010; 107:7431–7436. [PubMed: 20231459]
- Thompson MR, Kaminski JJ, Kurt-Jones EA, Fitzgerald KA. Pattern recognition receptors and the innate immune response to viral infection. *Viruses.* 2011; 3:920–940. [PubMed: 21994762]
- Untergasser A, Zedler U, Langenkamp A, Hosel M, Quasdorff M, Esser K, Dienes HP, Tappertzhofen B, Kolanus W, Protzer U. Dendritic cells take up viral antigens but do not support the early steps of hepatitis B virus infection. *Hepatology.* 2006; 43:539–547. [PubMed: 16496321]
- van den Broek MF, Muller U, Huang S, Aguet M, Zinkernagel RM. Antiviral defense in mice lacking both alpha/beta and gamma interferon receptors. *J Virol.* 1995; 69:4792–4796. [PubMed: 7609046]
- Villadangos JA, Young L. Antigen-presentation properties of plasmacytoid dendritic cells. *Immunity.* 2008; 29:352–361. [PubMed: 18799143]
- Wiesel M, Kratky W, Oxenius A. Type I IFN substitutes for T cell help during viral infections. *J Immunol.* 2011; 186:754–763. [PubMed: 21160039]
- Zhou S, Cerny AM, Zacharia A, Fitzgerald KA, Kurt-Jones EA, Finberg RW. Induction and inhibition of type I interferon responses by distinct components of lymphocytic choriomeningitis virus. *J Virol.* 2010; 84:9452–9462. [PubMed: 20592086]
- Zhou S, Kurt-Jones EA, Mandell L, Cerny A, Chan M, Golenbock DT, Finberg RW. MyD88 is critical for the development of innate and adaptive immunity during acute lymphocytic choriomeningitis virus infection. *Eur J Immunol.* 2005; 35:822–830. [PubMed: 15724245]
- Zinkernagel RM. Lymphocytic choriomeningitis virus and immunology. *Curr Top Microbiol Immunol.* 2002; 263:1–5. [PubMed: 11987811]
- Zucchini N, Bessou G, Robbins SH, Chasson L, Raper A, Crocker PR, Dalod M. Individual plasmacytoid dendritic cells are major contributors to the production of multiple innate cytokines in an organ-specific manner during viral infection. *Int Immunol.* 2008; 20:45–56. [PubMed: 18000008]

- Zuniga EI, Liou LY, Mack L, Mendoza M, Oldstone MB. Persistent virus infection inhibits type I interferon production by plasmacytoid dendritic cells to facilitate opportunistic infections. *Cell Host Microbe*. 2008; 4:374–386. [PubMed: 18854241]
- Zuniga EI, McGavern DB, Pruneda-Paz JL, Teng C, Oldstone MB. Bone marrow plasmacytoid dendritic cells can differentiate into myeloid dendritic cells upon virus infection. *Nat Immunol*. 2004; 5:1227–1234. [PubMed: 15531885]

HIGHLIGHTS

- pDCs are early and productive targets of prototypic Old-world arenavirus.
- pDC IFN-I production is dissociated from intrinsic virus replication.
- TLR7 induces multi-cytokine producing pDCs and limits their viral load.
- TLR7 promotes full activation of innate and adaptive immune cells.

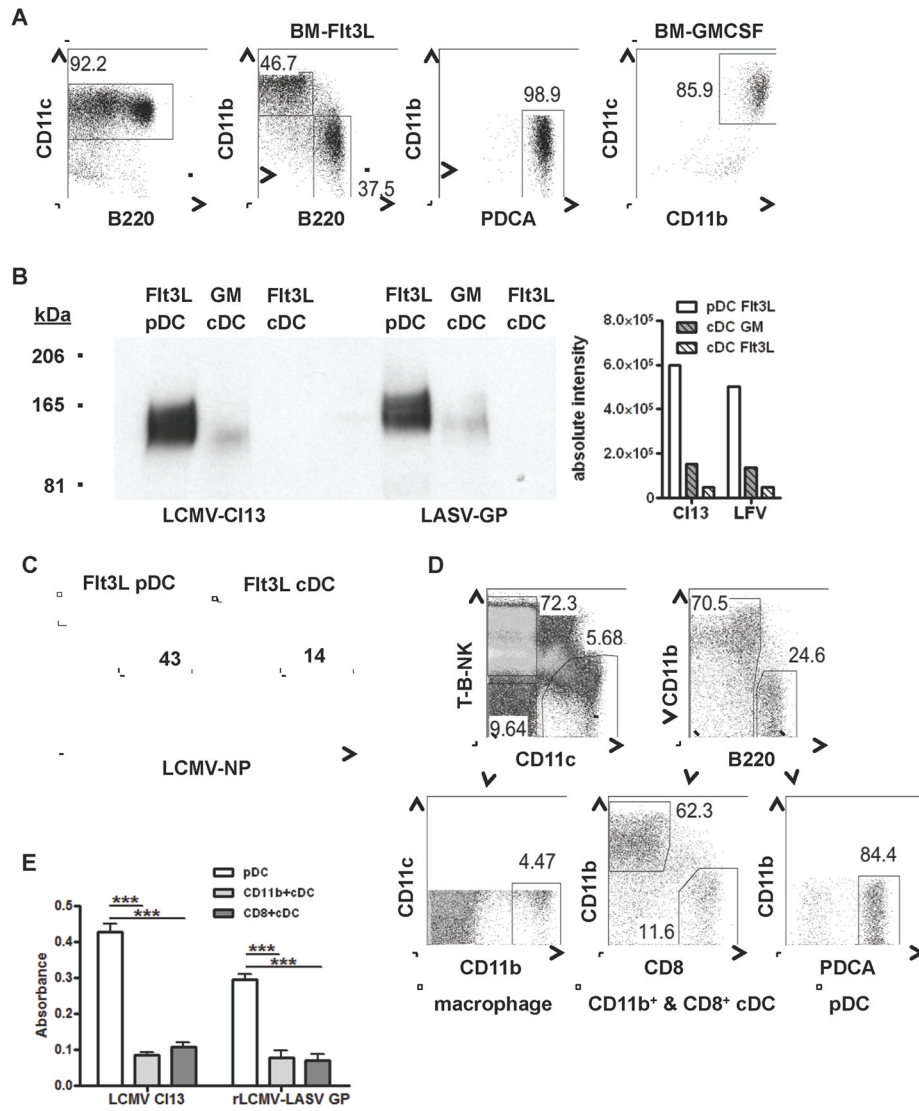


Figure 1. pDCs express high levels of Old-world arenavirus binding proteins

A–C. BM cells from uninfected (**A–B**) or day 3 LCMV CI13 infected mice (**C**) were cultured with GM-CSF to generate cDCs or Flt3L to generate pDCs and cDCs. **A.** At day 8–10 post-culture pDCs were identified as CD11c⁺CD11b⁻B220⁺PDCA⁺ and cDCs were identified as CD11c⁺CD11b⁺B220⁻ (Flt3L) and CD11c⁺CD11b⁺ (GM-CSF). **B.** pDCs and cDCs were processed for virus overlay assay with LCMV CI13 or LASV-GP. Virus binding to pDC or cDC protein homogenates is shown at 165kDa, similar to the molecular weight for α -DG. **C.** At day 4 post-culture Flt3L BM cultures were stained with anti-LCMV-NP Ab and analyzed by flow cytometry. Data are representative of 2–3 experiments. **D–E.** Splenic pDCs (T-B-NK⁻CD11c⁺CD11b⁻B220⁺PDCA⁺), CD11b⁺ cDCs (T-B-NK⁻CD11c⁺CD11b⁺B220⁻), and CD8⁺cDCs (T-B-NK⁻CD11c⁺CD11b⁻B220⁻CD8⁺) (**D**) were purified from uninfected mice and protein lysates were analyzed for LCMV CI13 and LASV GP (rLCMV-LASV GP) binding, measured by virus binding assay (**E**). Spleens were pooled from 5 mice in 2 independent experiments. Bar graphs depict the mean \pm SD. *p<0.05, **p<0.001, ***p<0.0001.

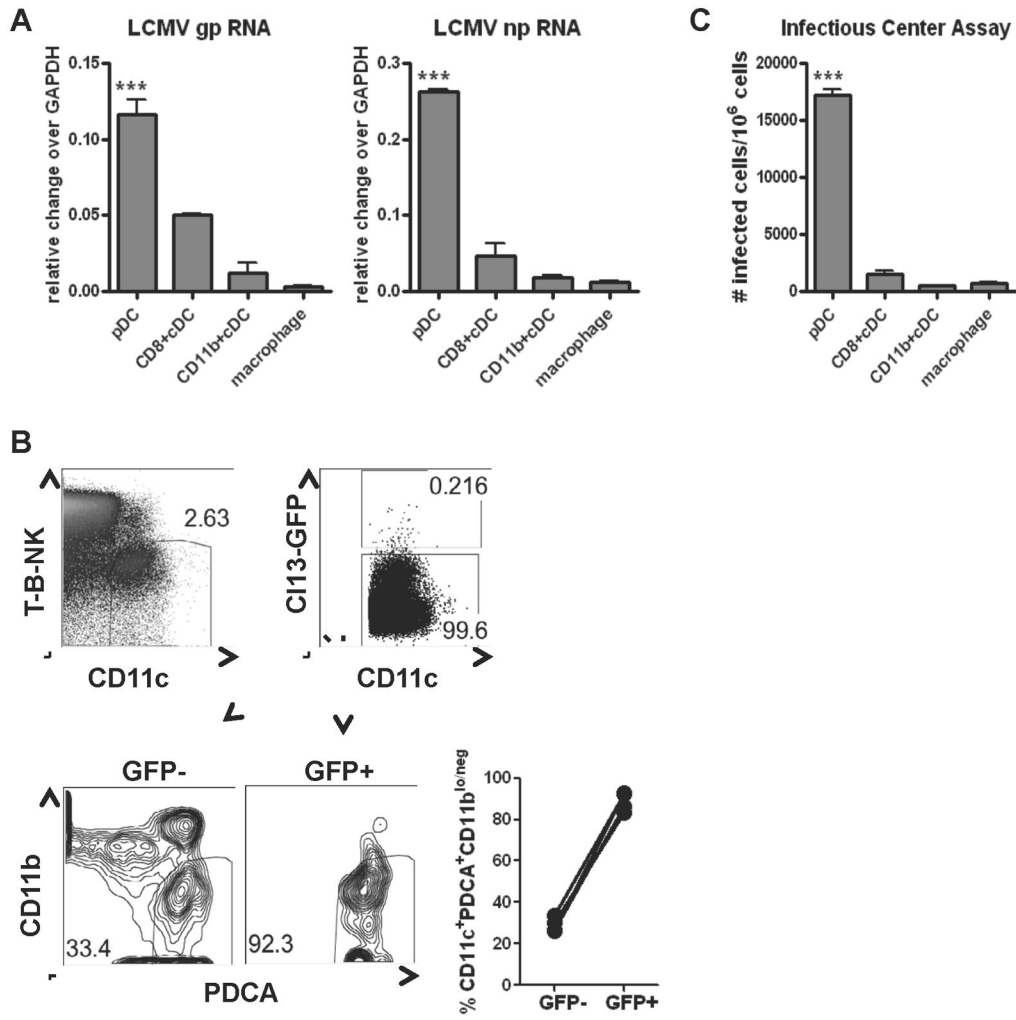


Figure 2. Rapid and productive pDC infection by LCMV CI13 *in vivo*

C57Bl/6 (WT) mice were infected with WT LCMV CI13 (A&C) or r3LCMVCI13-GFP (CI13-GFP; B). Spleens were pooled from 3–5 mice per group at day 1 p.i. and processed for FACS purification of pDCs, CD8⁺ and CD11b⁺ cDCs, and macrophages as described in figure 1D. **A.** LCMV *gp* and *np* RNA levels were determined relative to *gapdh* by qPCR. Bar graph depicts the mean±standard deviation (SD) of triplicates. **B.** The percentage of CD11c⁺PDCA⁺CD11b^{lo/neg} cells within GFP⁺ and GFP⁻ DCs was evaluated by flow cytometry. Representative plots are shown. Graph depicts the percentage of PDCA⁺CD11b^{lo/neg} cells within DC gate, where circles represent individual mice. **C.** Infectious center assay determined the number of productively infected cells per million cells. Bar graphs depict the mean±SD. All results are representative of 3–4 experiments with 3–5 mice/group. p<0.05, **p<0.001, ***p<0.0001. See also Figure S1.

and infected mice are shown. Bar graphs depict percentage of IL-12p40⁺ and TNFα⁺ cells. **E.** YFP⁺ splenocytes from IFNβ^{mob/mob} infected mice were analyzed for IL-12p40 and TNFα expression by flow cytometry. Representative dot plots are shown. Bar graphs depict percentage of IL-12p40⁺ and TNFα⁺ cells within YFP⁺ cells. All bar graphs depict mean ±SD and data are representative of 2–3 experiments with 4–5 mice/group. *p<0.05, **p<0.001, ***p<0.0001. See also Figure S2.

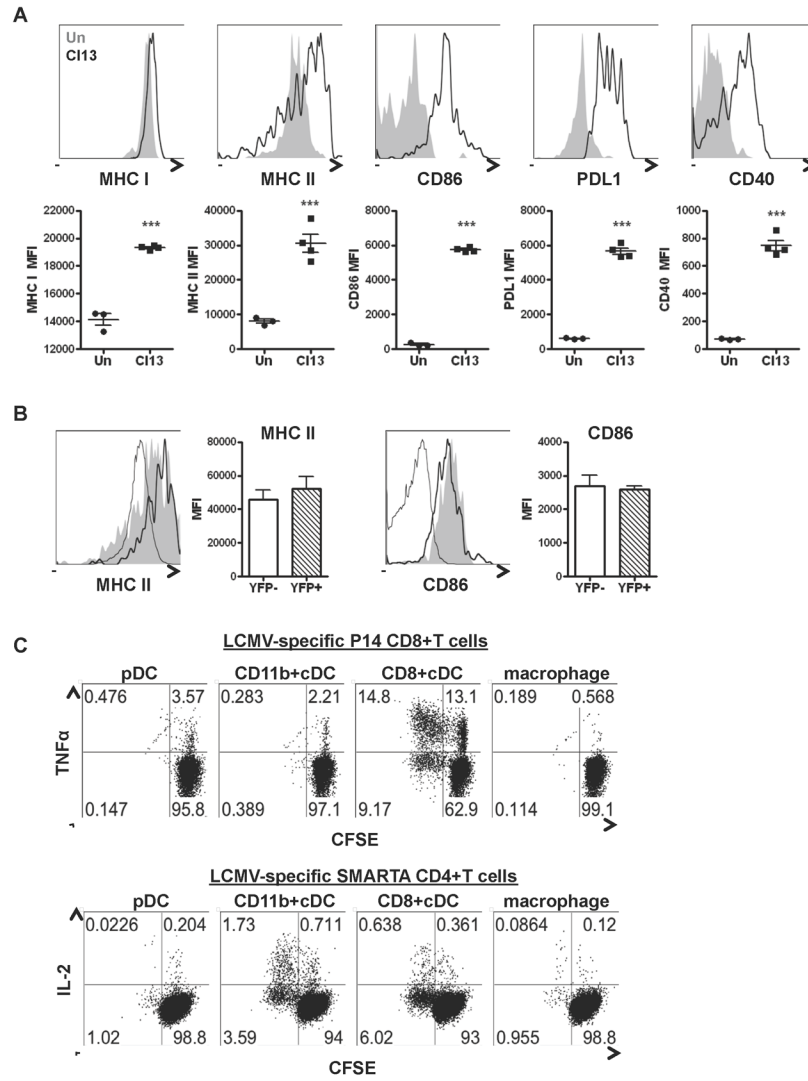


Figure 4. pDCs matured but remained poor antigen presenting cells during LCMV CI13 infection

WT (A–C) and IFN $\beta^{\text{mob/mob}}$ (B) mice were left uninfected or infected with LCMV CI13 and splenocytes were obtained at day 1 p.i. **A.** MHC I, MHC II, CD86, PDL1 and CD40 expression in pDCs was determined by flow cytometry. Representative histograms of uninfected (gray solid) and infected (black unfilled) mice are shown. Graphs depict mean \pm SD of mean fluorescence intensity (MFI) for indicated molecules, where symbols represent individual mice **B.** MHC II and CD86 expression was analyzed by flow cytometry in YFP⁻ and YFP⁺ pDCs from IFN $\beta^{\text{mob/mob}}$ infected mice. Representative histograms for uninfected pDC (gray unfilled) and infected YFP⁻ (gray solid) and YFP⁺ (black unfilled) pDCs are shown. Bar graphs depict mean \pm SD of MFI for indicated molecules **C.** pDCs, CD11b⁺ and CD8⁺cDCs, and macrophages were FACS-purified from pooled splenocytes of infected mice and co-cultured with CFSE-labeled naïve P14 CD8⁺ or SMARTA CD4⁺ T cells for 72hrs. T cells were analyzed for proliferation (CFSE⁻) and TNF α or IL-2 production by P14 and SMARTA cells, respectively. All results are representative of 2–4 experiments with 4–5 mice/group. * $p < 0.05$, ** $p < 0.001$, *** $p < 0.0001$. See also Figure S3.

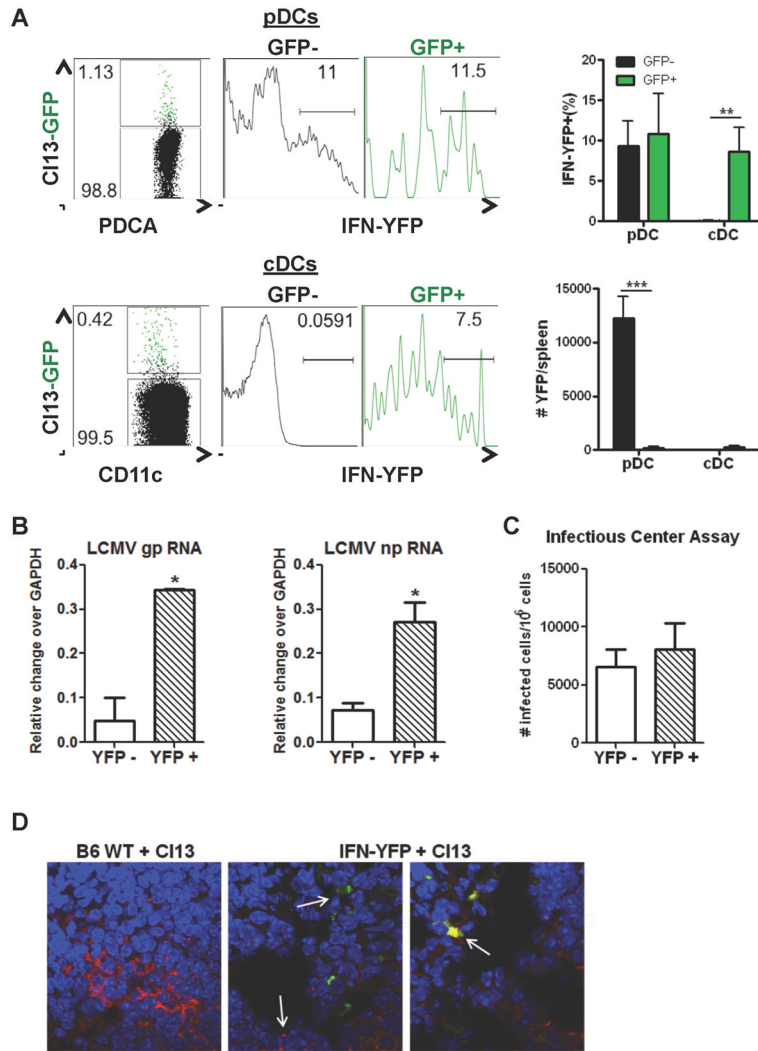


Figure 5. pDC produce IFN-I independent of intrinsic LCMV CI13 replication

WT or IFN $\beta^{mob/mob}$ mice were left uninfected or infected with either CI13-GFP (A) or WT LCMV CI13 (B–D) and spleens were processed at day 1 p.i. A. YFP signal was analyzed by flow cytometry in infected (GFP⁺) and uninfected (GFP⁻) PDCA enriched pDCs and cDCs. Representative dot plots are shown. B–C. Spleens were pooled from 4–5 mice/group for FACS purification of YFP⁺ and YFP⁻ pDCs. LCMV *gp* and *np* RNA transcript levels were determined relative to *gapdh* (B). Productively infected YFP⁺ vs. YFP⁻ pDCs were quantified by infectious center assay (C). Bar graphs represent mean \pm SD. D. Spleens were evaluated for IFN β (green) and LCMV CI13 (red) localization by confocal microscopy. Nuclei are stained with DAPI (blue). White arrows indicate IFN β producing and CI13-infected cells (middle panel) and double positive stained cells (right panel). All bar graphs depict mean \pm SD and results are representative of 2–3 independent experiments with 3–5 mice/group. * $p < 0.05$, ** $p < 0.001$, *** $p < 0.0001$. See also Figure S4.

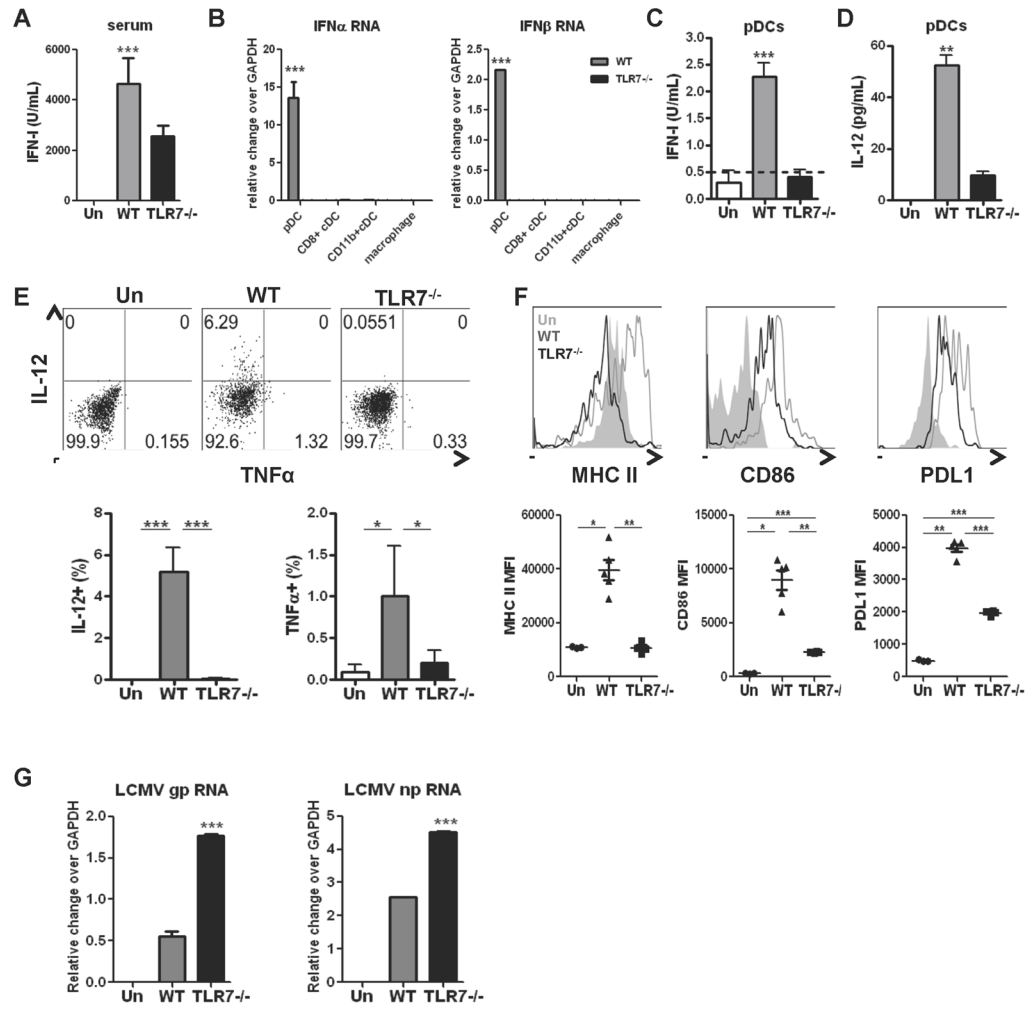


Figure 6. pDCs sense in vivo LCMV CI13 infection through TLR7

WT or TLR7^{-/-} mice were left uninfected or infected with WT LCMV CI13 and serum (A) or spleens (B–G) were processed at day 1 p.i. A. Serum IFN-I activity was measured by luciferase bioassay. B–D. pDCs, CD11b⁺ and CD8⁺ cDCs, and macrophages were FACS-purified from spleens pooled from 4–5 mice per group. *Ifna* and *Ifnb* transcript levels were determined relative to *gapdh* by qPCR (B). pDCs were cultured and supernatants collected at 15 hrs to measure IFN-I bioactivity, where dotted line indicates limit of bioassay detection (C), or IL-12p70 levels (D). E. The percentage of IL-12p40⁺ and TNF α ⁺ pDCs was determined by flow cytometry. Representative dot plots are shown. F. MHC II, CD86, and PDL1 expression were analyzed in pDCs by flow cytometry. MFI \pm SD are graphed where symbols represent individual mice. Representative histogram of uninfected (gray solid), and CI13 infected WT (gray unfilled) and TLR7^{-/-} (black unfilled) mice are shown. G. LCMV *gp* and *np* transcripts were quantified in FACS-purified pDCs by qPCR. All bar graphs depict mean \pm SD and data are representative of 2–3 independent experiments with 3–5 mice/group. *p<0.05, **p<0.001, ***p<0.0001.

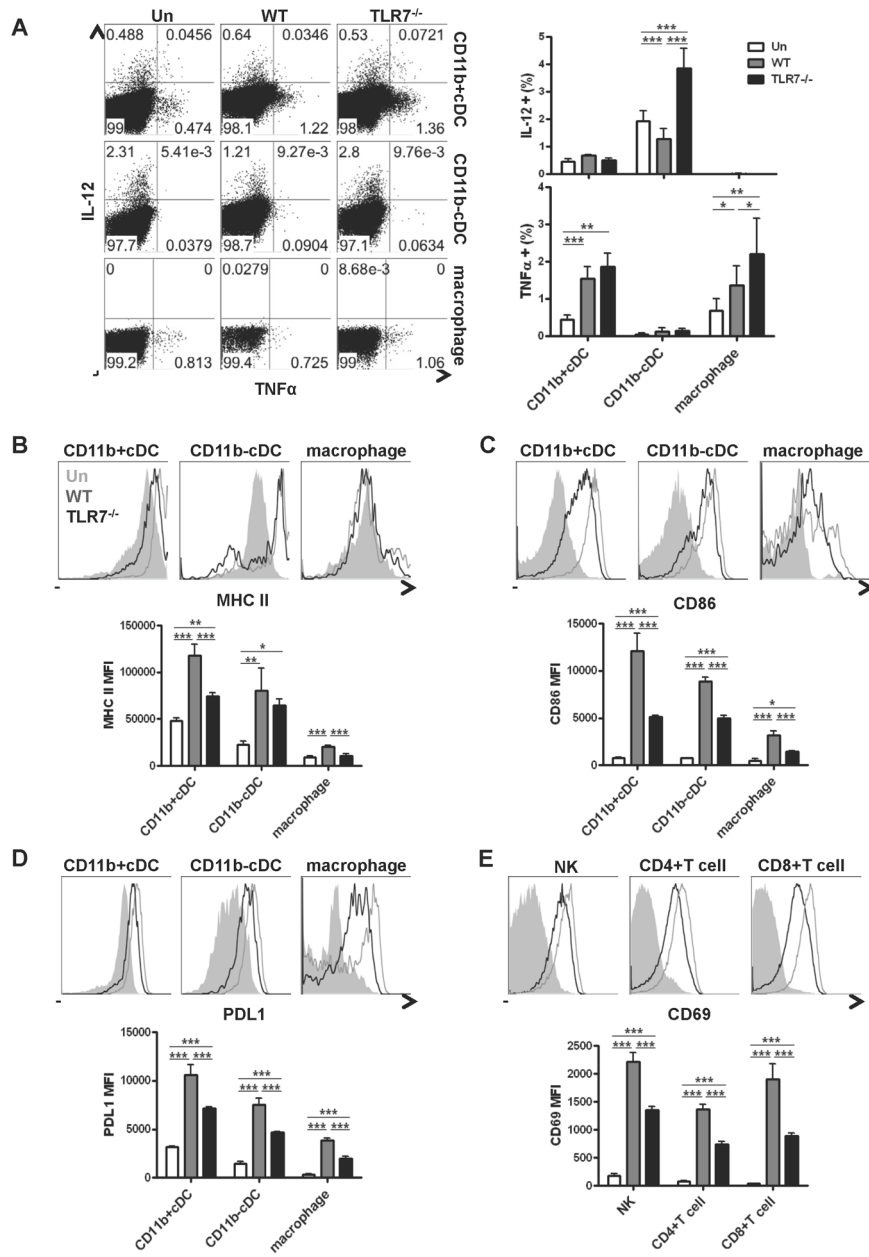


Figure 7. TLR7 mediates early activation of innate and adaptive immune cells
 WT or TLR7^{-/-} mice were left uninfected or infected with WT LCMV C113 and spleens were processed at day 1 p.i. **A.** The percentage of IL-12⁺ and TNFα⁺ CD11b⁺ and CD11b⁻cDCs, and macrophages was determined by flow cytometry. Representative dot plots are shown. Bar graph depicts mean ± SD. **B–D.** MHC II, CD86, and PDL1 expression were analyzed in CD11b⁺cDCs (**B**), CD11b⁻cDCs (**C**), and macrophages (**D**) by flow cytometry. **E.** NK, CD4⁺ and CD8⁺T cells were analyzed by flow cytometry for expression of CD69. Representative histogram of uninfected (gray solid), and C113 infected WT (gray unfilled) and TLR7^{-/-} (black unfilled) mice are shown. Graphs depict mean MFI±SD. All results are representative of 3–4 independent experiments with 3–5 mice/group. *p<0.05, **p<0.001, ***p<0.0001